Prompt photons + jet in DIS

P. Bussey, O. Hlushchenko,

D. Saxon, I. Skillicorn

9 March 2016

Physics overview

- Kinematics:
  - $Q^2 = -q^2$ – virtuality
  - $y = \frac{P \cdot q}{P \cdot l}$ – inelasticity
  - $x = \frac{Q^2}{2P \cdot q}$ – longitudinal momentum fraction carried by the incoming parton

Electron/Positrons: 27.5 GeV
Protons: 920 GeV
Luminosity of ~ 326 pb^{-1}

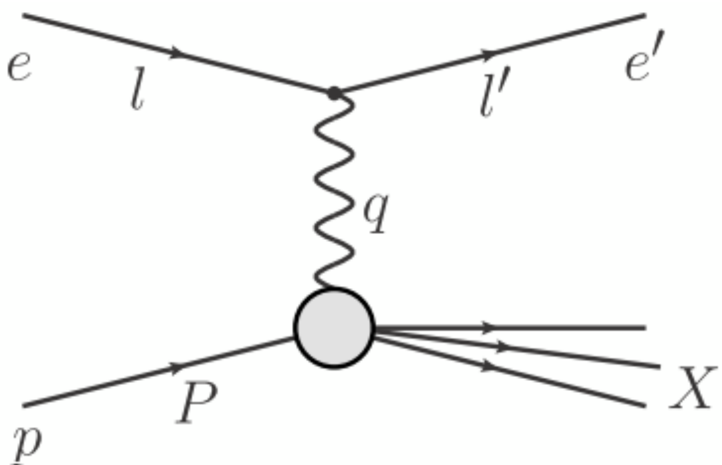

Data
- 0405e, 06e, 0607p

MC
- PYTHIA (signal) - unfortunately we do not have Herwig for this
- ARIADNE (background)

Prompt photons

- Photons which are produced promptly in the collision, **before the quarks and gluons have had time to form hadrons, and well before those hadrons decay**
- High transverse energy final state photons (E_T^{γ})
- Isolated state:
  - no tracks within $\Delta R(\eta, \varphi) = 0.2$ cone around the photon candidate
  - photon candidate in jet has >=90% of jet energy

QQ - photons

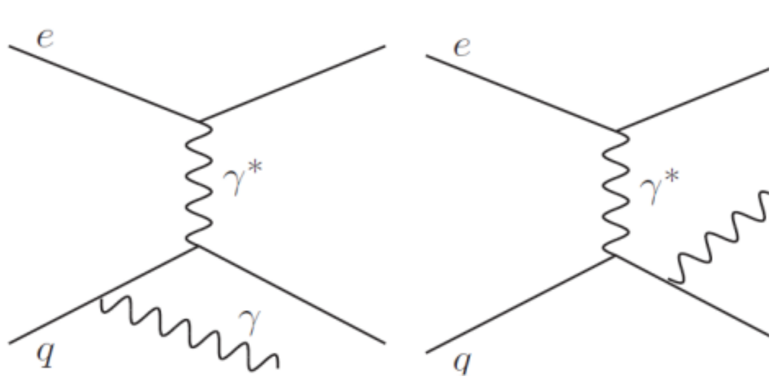

prompt photons are emitted from a quark as part of a QCD process (QQ photons)

LL - photons

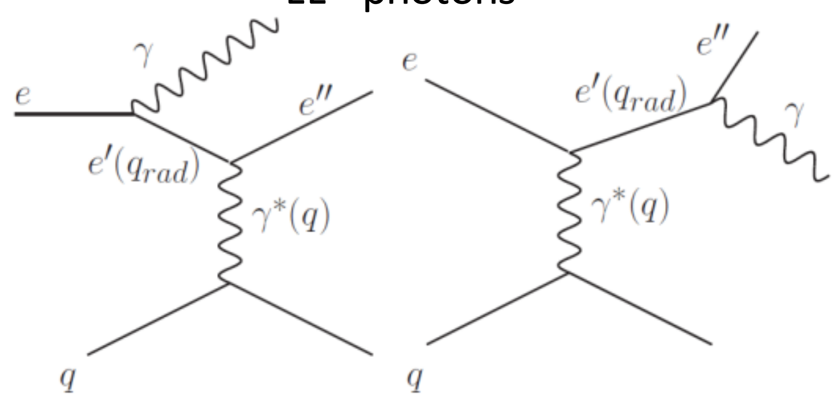

photon is radiated from an incoming or outgoing lepton (LL photons)

Event selection

- DIS selection
  - $10 < Q^2_{el} < 350\, GeV^2$
  - Electron cuts:
    - $E_{e,corr} > 10\ GeV$
    - $140^o < \theta_{el} < 180^o$
    - $|X| < 14.8, cm$
    - $|Y| < 14.8, cm$
- Prompt photon selection
  - $4 < E_T^{\gamma} < 15, GeV$
  - $-0.7 < \eta_{\gamma} < 0.9$
  - $E_{\gamma} \div E_{jet\ with\ \gamma} > 0.9$
  - $\Delta R < 0.2$ – no tracks
  - $E_{EMC} \div (E_{EMC} + E_{HAC})$
- Jet selection (zufos used)
  - $E_T^{jet} > 2.5, GeV$
  - $-1.5 < \eta_{jet} < 1.8$
  - Use jet with $E^{jet}_{T,max}$
- Cleaning
  - Triggers
    - SPP02 for 0405e
    - SPP09 for 06e, 0607p
  - $|Z_{vtx}| < 40, cm$
  - $35 < E - p_z < 65, GeV$
  - Number of vertex tracks not in RCAL > 1

Jet construction

- *Electron* is not used in jet finding
- k_T-clustering alg. from *KtJet* is used (R=1)
- Jet which is recognized as containing the photon candidate is excluded
- Highest-E_T^{jet} that does not contain the photon candidate and passes the cuts is treated accompanying hadronic jet

Observables to study

- $x_\gamma = \frac{\sum_{jet,\gamma}(E-p_z)}{2y_{Bj}E_e}$
- $\Delta\eta_{\gamma,jet} = \eta_{jet} - \eta_\gamma$
- $\Delta\eta_{\gamma,e} = \eta_e - \eta_\gamma$
- $x_p = \frac{\sum_{jet,\gamma}(E+p_z)}{2E_p}$
- $\Delta\varphi_{\gamma,jet} = \varphi_{jet} - \varphi_\gamma$
- $\Delta\varphi_{e,\gamma} = \varphi_e - \varphi_\gamma$

Similar kind of analysis was previously done for photoproduction (Q^2<1) for variables $\Delta\eta$, $\Delta\psi$, x_γ, x_p

<u>What was done:</u>

- Moved to new fitting region – excluding the first bin from the fit
- Corrected signal shape
- Studied new ways of doing the fit
- Recalculated and compared new cross sections

Signal extraction

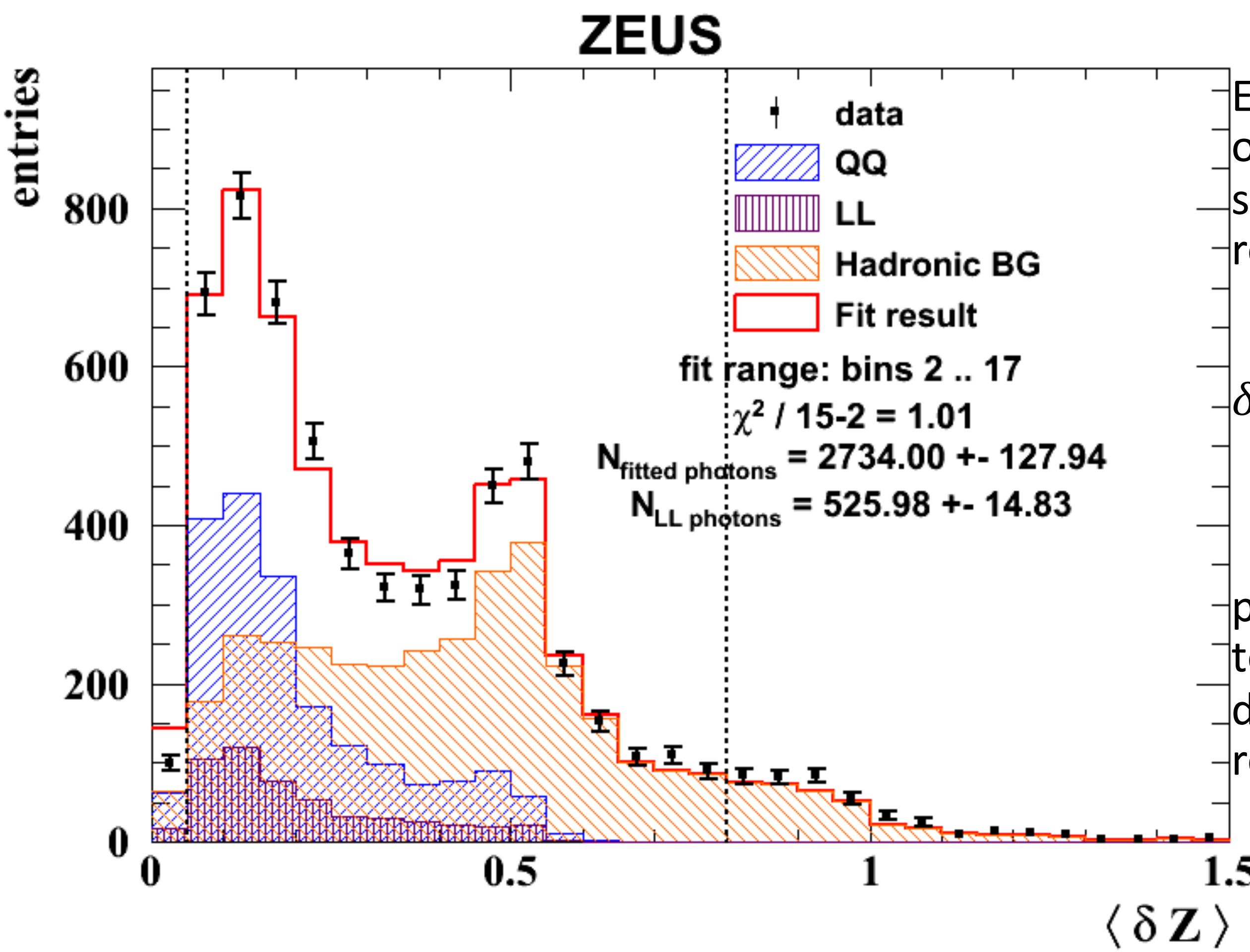

Energy-weighted mean width of the electromagnetic shower(cluster) in calorimeter relative to its centroid:

$$\delta Z = \frac{\sum_{zufo} |z_i - z_{cluster}| \cdot E_i}{l_{cell} \sum E_i}$$

Number of fitted photons increased compared to 2440±60 . This is mostly due to changing the fitting region.

Signal-shape correction

- The fit became better overall
- Number of fitted photons decreased to 2734
- For DVCS, the deviation between the MC and data is confined to the peak of the distribution therefore only 3 bins of the signal are corrected.

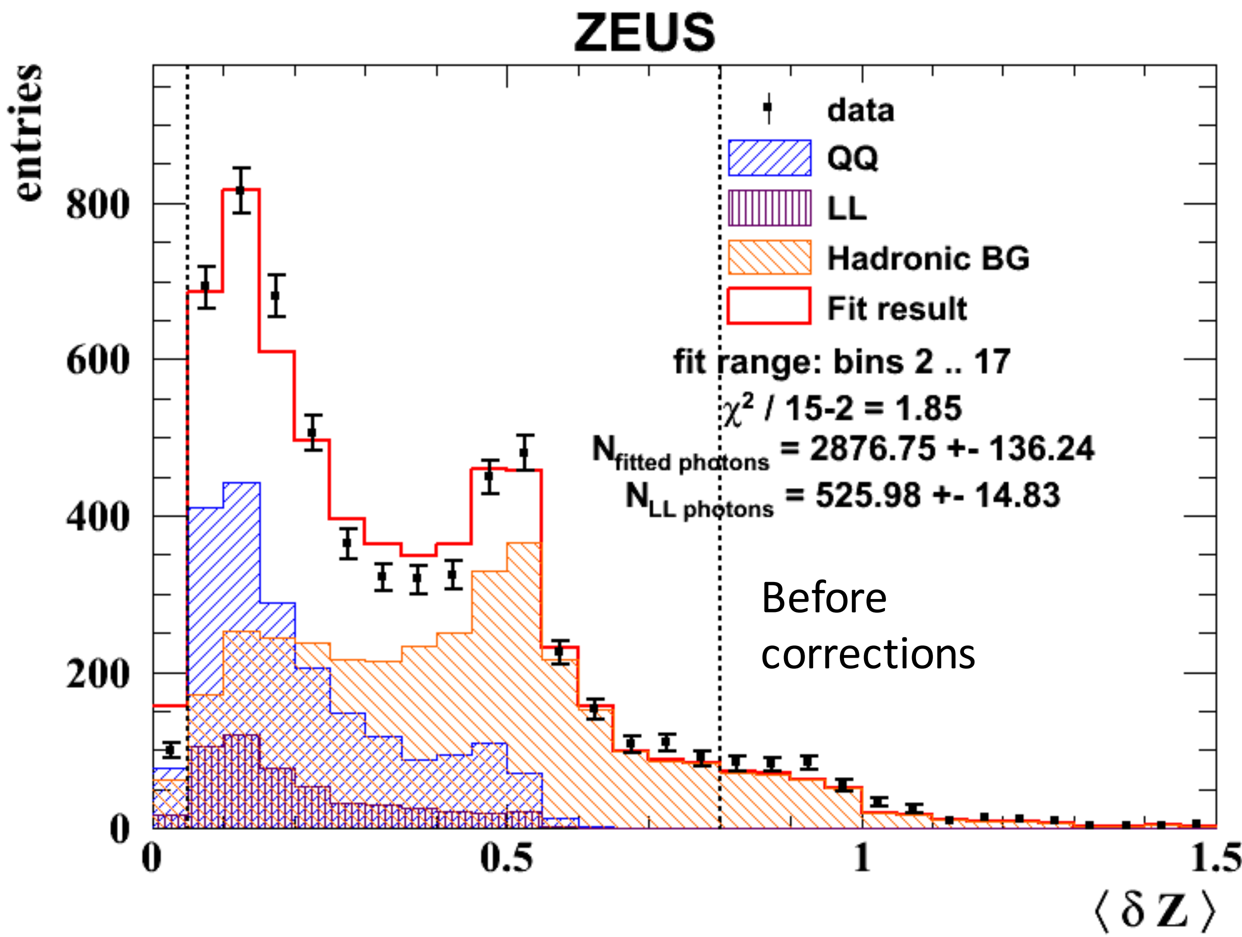

See DVCS plots on http://www.ppe.gla.ac.uk/~skilli/photonjet.html

Acceptance

$Acc = \frac{N_{detector\ level}}{N_{true\ level}}$ -relation of corresponding histograms scaled to data luminosity

Values above 1 due to bin-by-bin migration

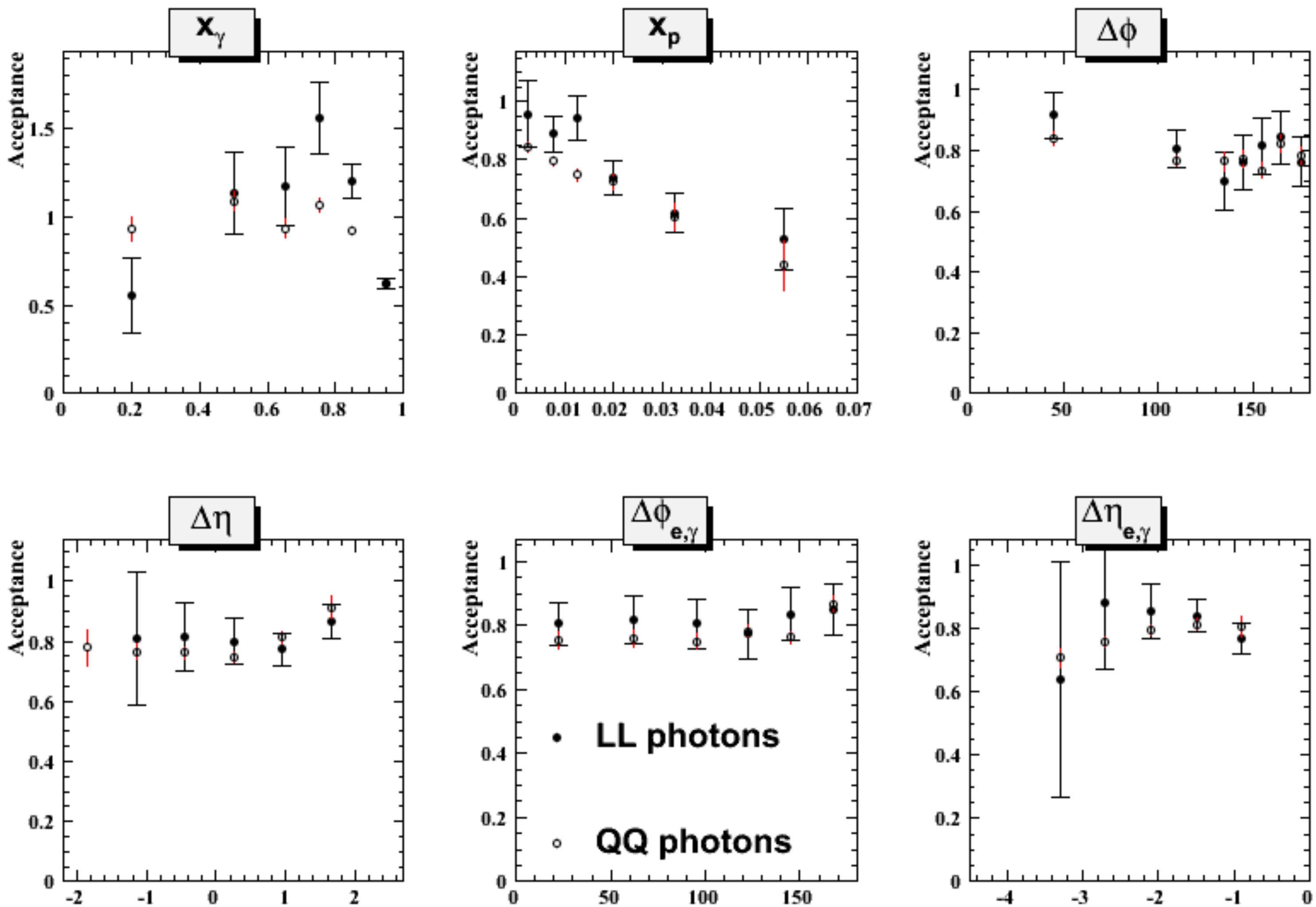

Purity

is defined as the relation of found with detector level cuts photons to actual photons

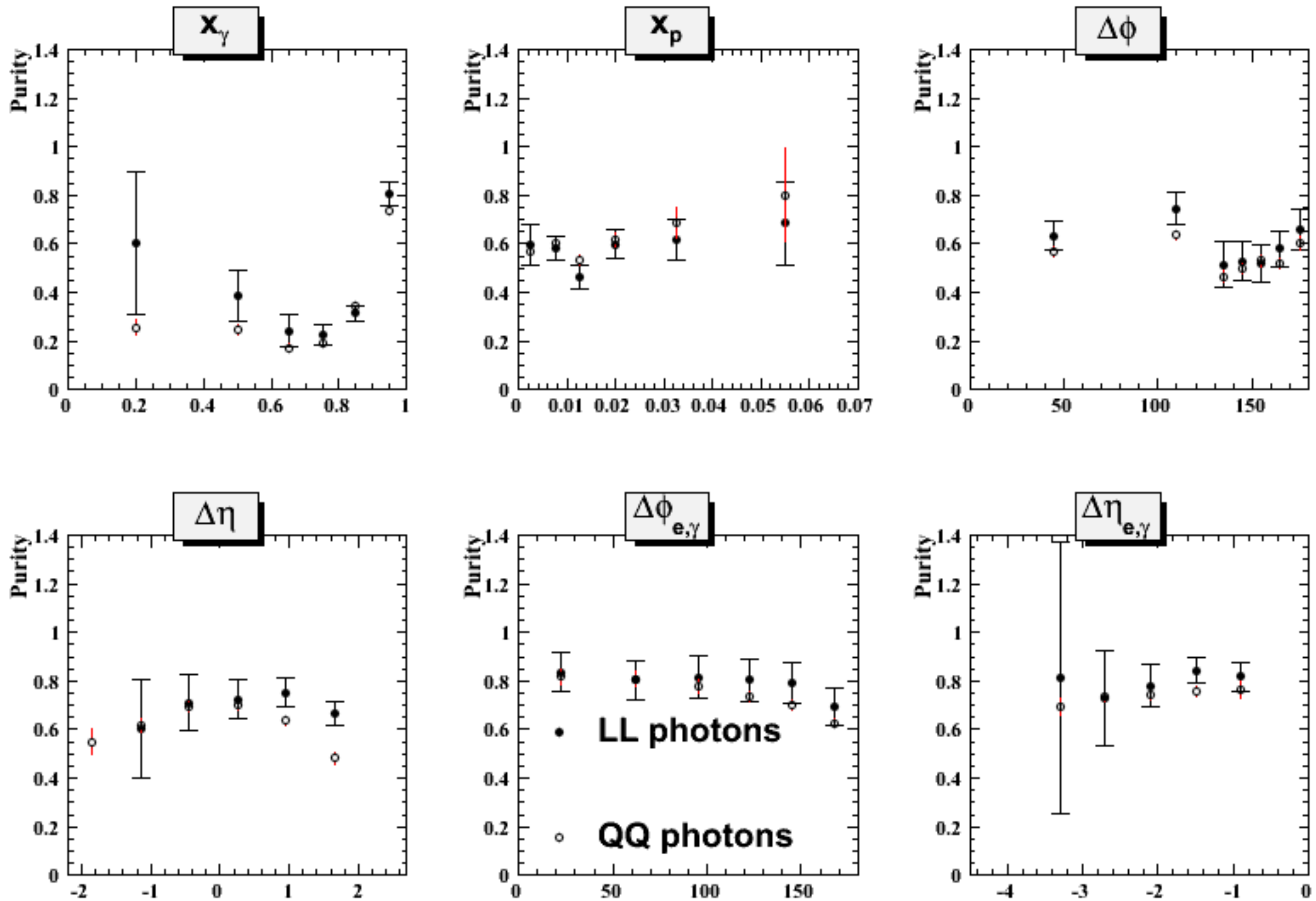

Errors

- Errors sources:
  - δLuminosity – neglected
  - δN – statistical errors on QQ and LL MC sampes
  - δacc – acceptance errors
  - δa – errors of found fit parameter
- Before applying cuts for the event selection the values of such variables as:
  - E_γ - energy of the photon
  - E_{jet}- energy of the jet
  - E_e- energy of the electron

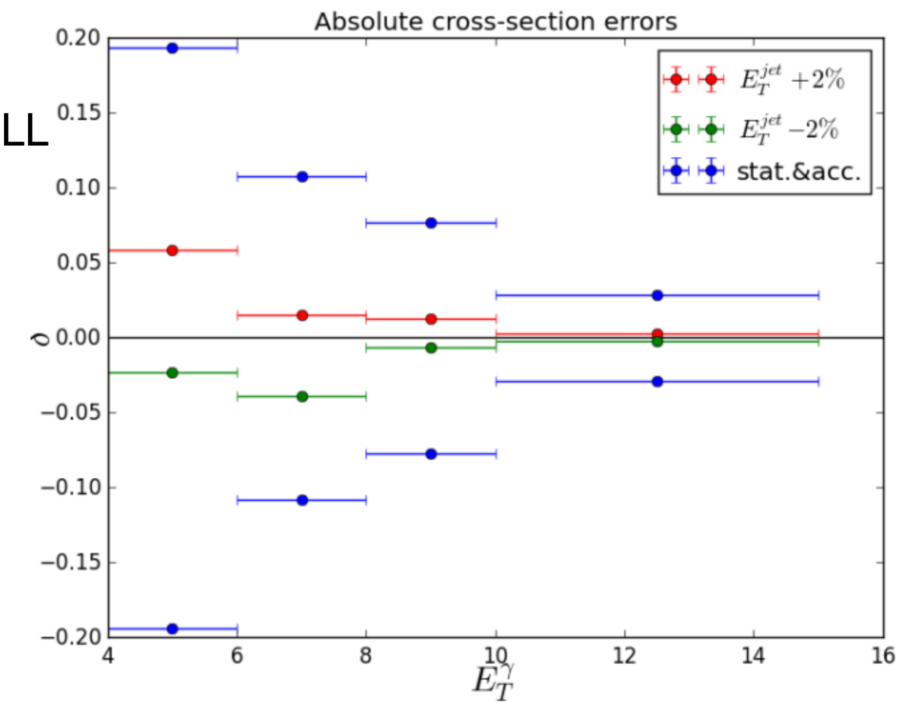

are corrected to $\pm 2\%$ and the cross sections are recalculated (one by one, both for MC and Data)

- The obtained CS are then compared to one we calculated previously without any corrections

Cross sections

- For a given observable Y ,
  the production
  cross section:

$$\frac{d\sigma}{dY} = \frac{A_{QQ} \cdot N(\gamma_{QQ})}{\mathcal{L} \cdot \Delta Y} + \frac{d\sigma_{LL}^{MC}}{dY}$$

  $N(\gamma_{QQ})$ - number of QQ photons extracted from the fit,
  ΔY - bin width,
  $\mathcal{L}$ -total integrated luminosity,
  σ_{LL}^{MC} - cross section for LL photons

- $A_{QQ} = \frac{N_{detector\ level}}{N_{true\ level}}$ - acceptance correction for QQ photons
- Good agreement with the published results

Comparison with article

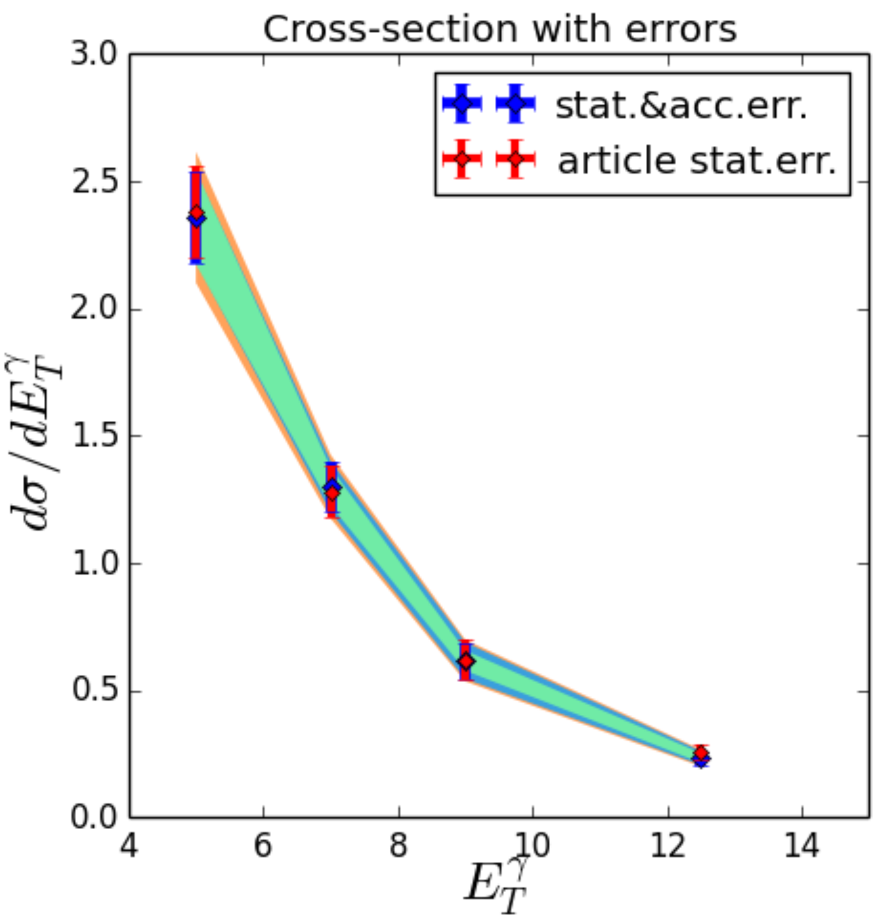

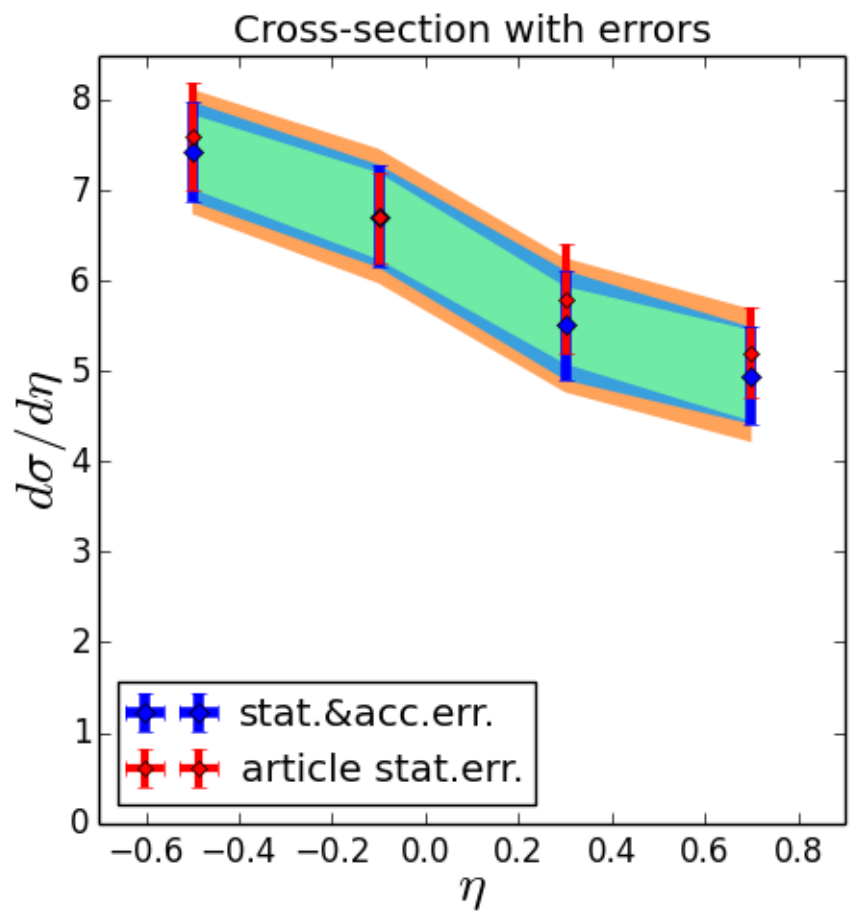

Comparison with article

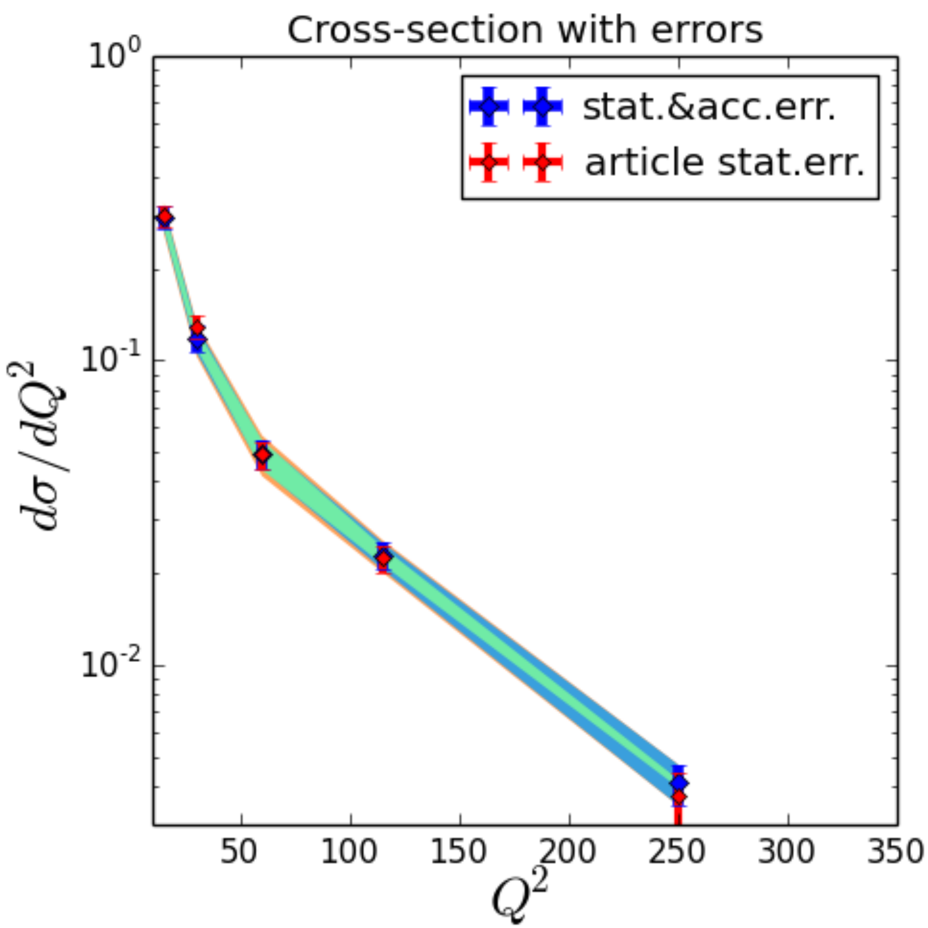

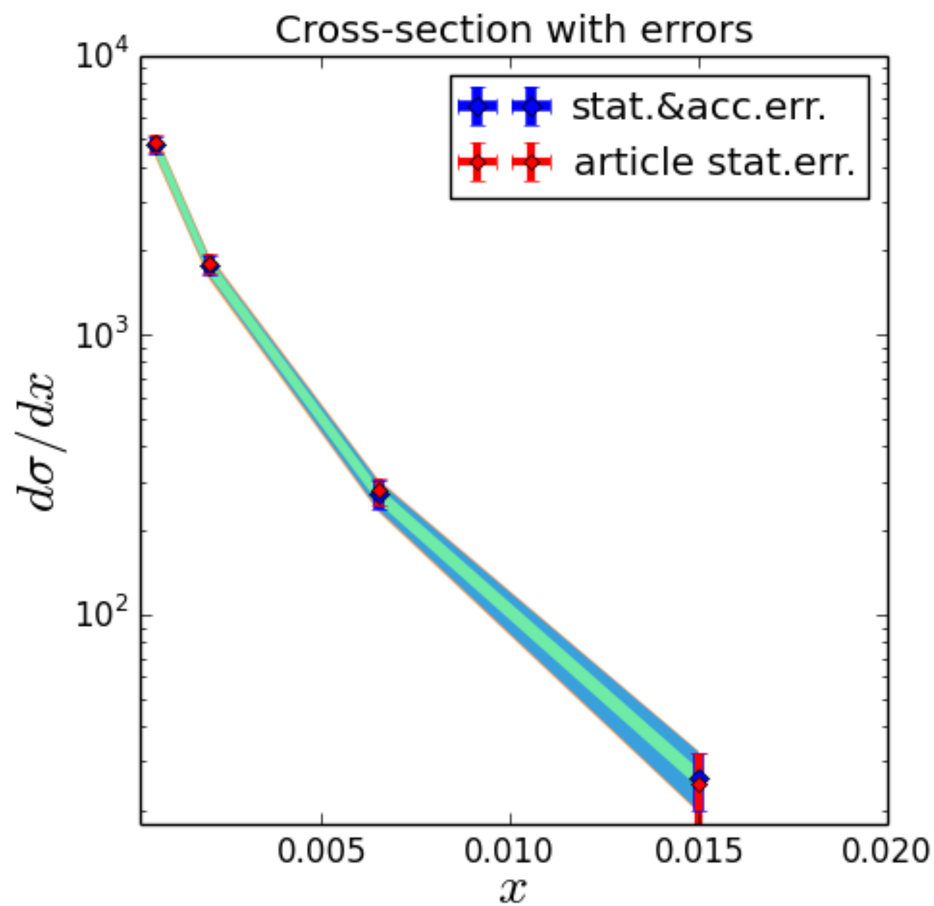

Comparison with article

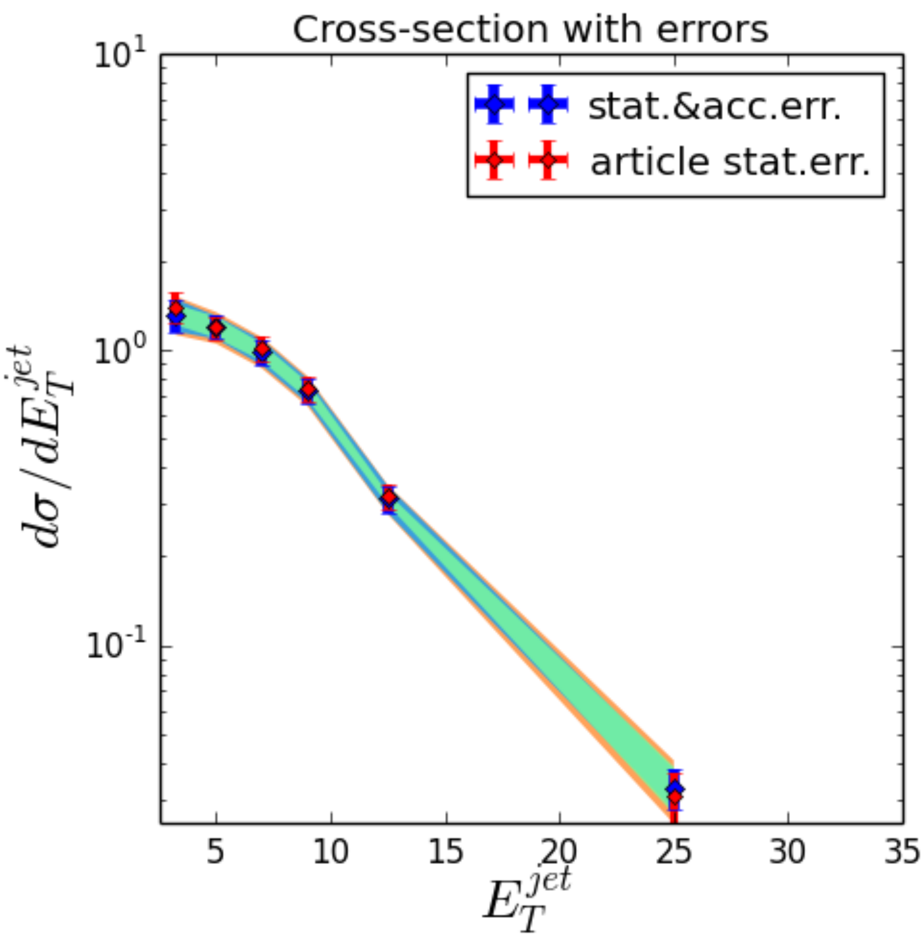

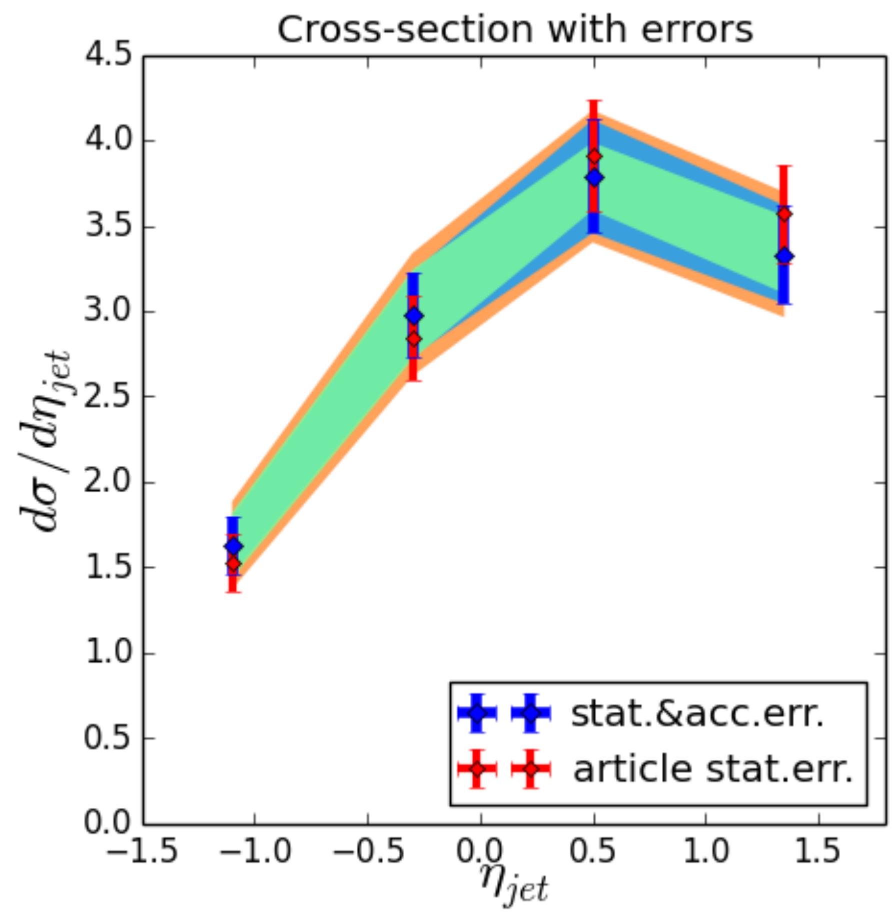

Preliminary

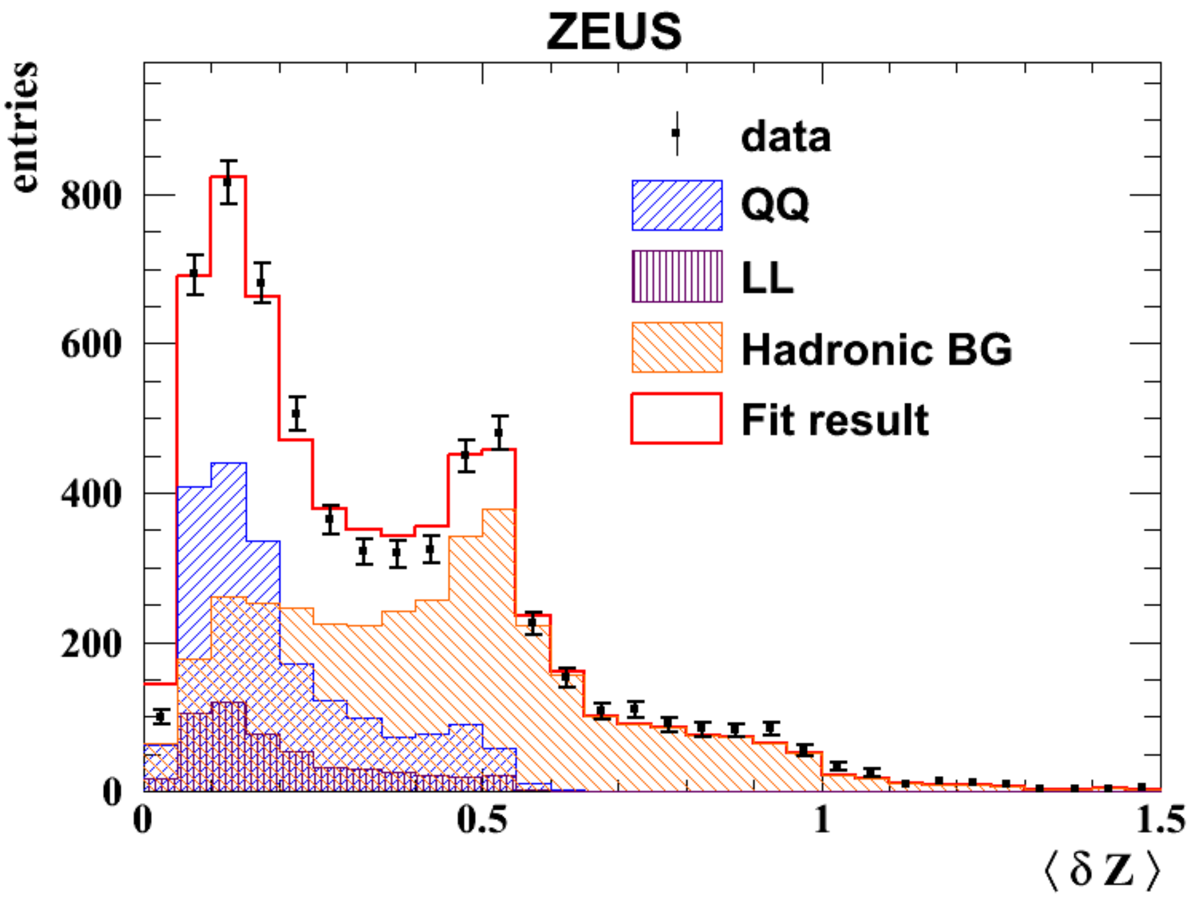

Preliminary

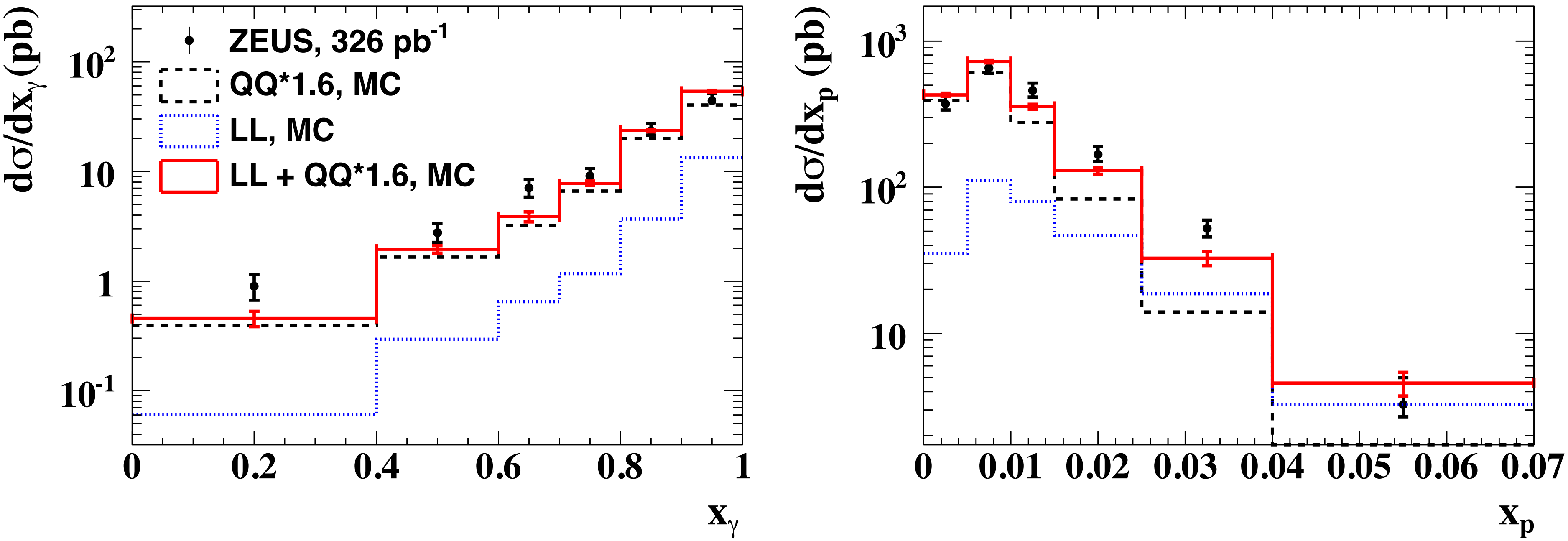

Preliminary

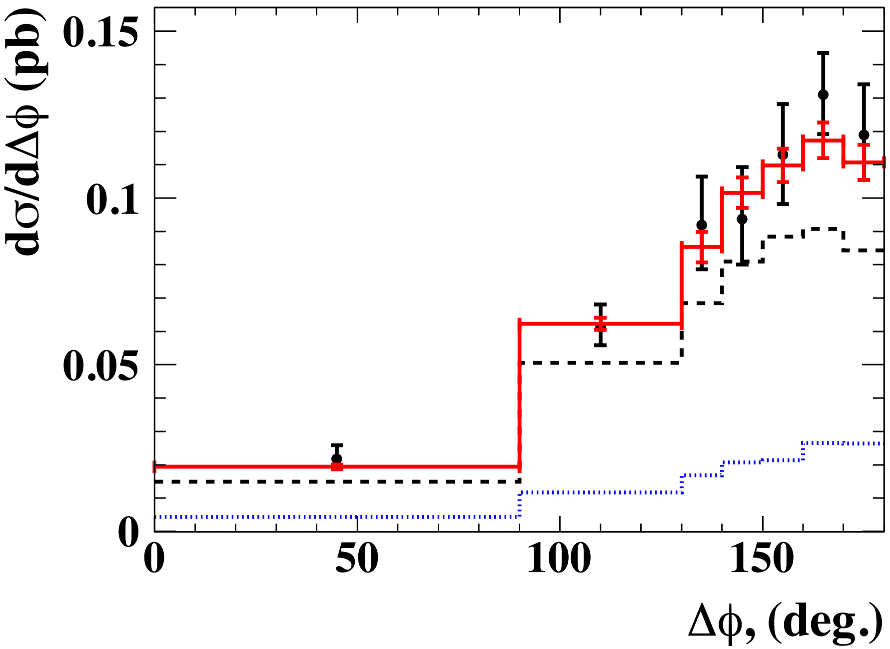

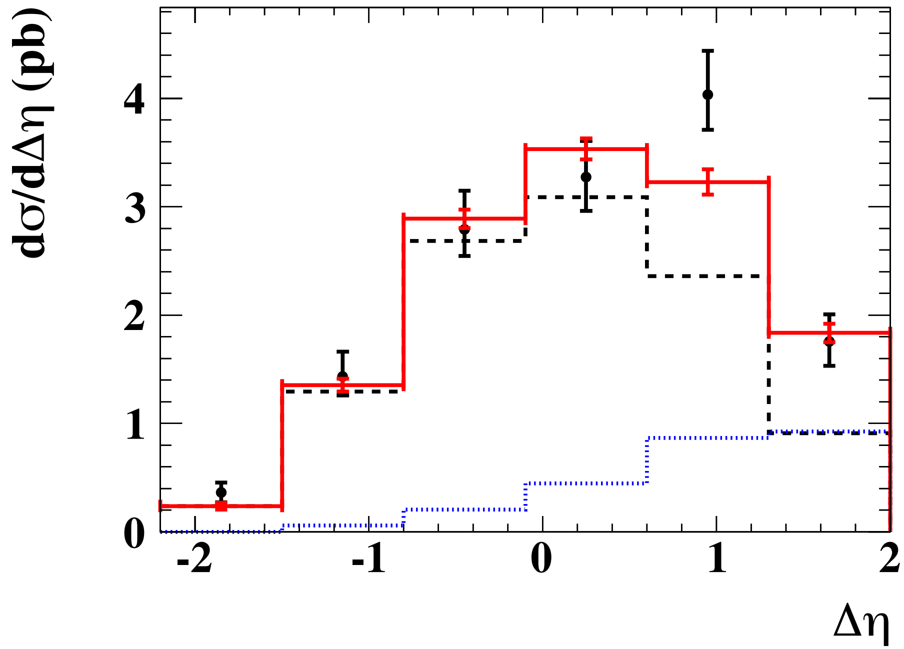

Preliminary

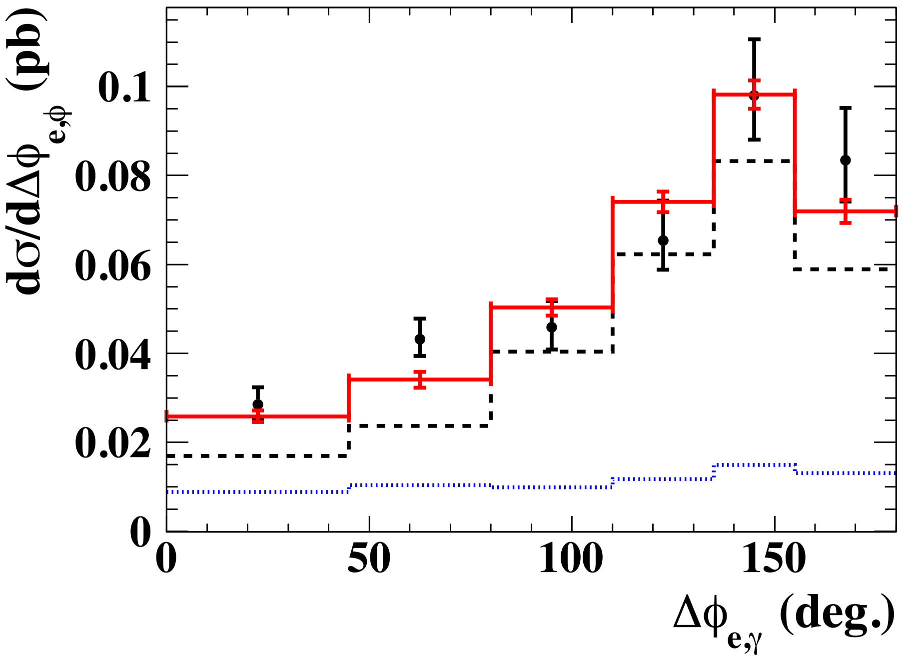

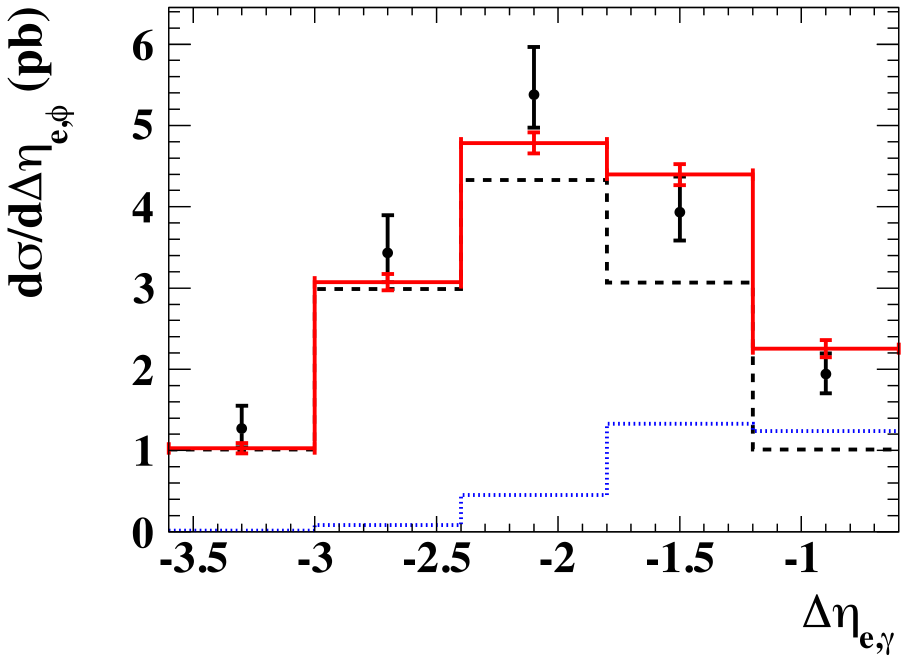

Conclusions

- We confirmed the previous published paper results
- Cross sections were built in different regions of new observables of interest e.g. $\Delta\eta$, $\Delta\psi$, $\Delta\psi_{e,\gamma,}$, x_γ, x_p, similar as it was done for photoproduction
- unfolding instead of bin-by-bin correction – might be not enough MC but can make the acceptance better
- We have asked the theorist for the calculations and we wait for their replies

Appendix. Total cross section

- variable E_T^{γ} σ_{tot} = 9.7283 +- 0.4152 pb Prev. paper was 9.86 +/- 0.45 pb
- variable η_{γ} σ_{tot} = 9.84094 +- 0.411581 pb
- variable Q^2 σ_{tot} = 9.68468 +- 0.411113 pb
- variable x σ_{tot} = 9.51108 +- 0.415857 pb
- variable E_T^{jet} σ_{tot} = 10.0189 +- 0.407521 pb
- variable η_{jet} σ_{tot} = 9.71037 +- 0.389135 pb
- variable x_{γ} σ_{tot} = 9.29195 +- 0.331309 pb
- variable x_p σ_{tot} = 9.98807 +- 0.417831 pb
- variable $\Delta\varphi$ σ_{tot} = 9.89287 +- 0.408290 pb
- variable $\Delta\eta$ σ_{tot} = 9.55389 +- 0.371788 pb
- variable $\Delta\varphi^{e,\gamma}$ σ_{tot} = 9.85318 +- 0.391102 pb
- variable $\Delta\eta^{e,\gamma}$ σ_{tot} = 9.57181 +- 0.402304 pb

Appendix. Paper CS

E_T^γ range (GeV)	$\frac{d\sigma}{dE_T^\gamma}$ (pb GeV^{-1})	New CS
4–6	2.38 ± 0.18 (stat.) ± 0.13 (sys.)	2.490760 +- 0.1936(stat.) +- 0.1512(sys.)
6–8	1.28 ± 0.10 (stat.) ± 0.06 (sys.)	1.347580 +- 0.1083(stat.) +- 0.0708(sys.)
8–10	0.62 ± 0.08 (stat.) ± 0.04 (sys.)	0.655572 +- 0.0768(stat.) +- 0.0385(sys.)
10–15	0.26 ± 0.03 (stat.) ± 0.02 (sys.)	0.251853 +- 0.0284(stat.) +- 0.0215(sys.)

η^γ range	$\frac{d\sigma}{d\eta^\gamma}$ (pb)	New CS
−0.7 to −0.3	7.6 ± 0.6 (stat.) ± 0.5 (sys.)	7.687960 +- 0.5864(stat.) +- 0.3999(sys.)
−0.3–0.1	6.7 ± 0.5 (stat.) ± 0.3 (sys.)	6.902880 +- 0.5935(stat.) +- 0.4622(sys.)
0.1–0.5	5.8 ± 0.6 (stat.) ± 0.3 (sys.)	5.756020 +- 0.6272(stat.) +- 0.3228(sys.)
0.5–0.9	5.2 ± 0.5 (stat.) ± 0.4 (sys.)	5.318710 +- 0.5552(stat.) +- 0.4746(sys.)

Q^2 range (GeV^2)	$\frac{d\sigma}{dQ^2}$ (pb GeV^{-2})	New CS
10–20	0.298 ± 0.024 (stat.) ± 0.019 (sys.)	0.308169 +- 0.0267(stat.) +- 0.0202(sys.)
20–40	0.129 ± 0.012 (stat.) ± 0.009 (sys.)	0.126468 +- 0.0128(stat.) +- 0.0054(sys.)
40–80	0.049 ± 0.005 (stat.) ± 0.004 (sys.)	0.049957 +- 0.0054(stat.) +- 0.0044(sys.)
80–150	0.0224 ± 0.0023 (stat.) ± 0.0011 (sys.)	0.023656 +- 0.0024(stat.) +- 0.0015(sys.)
150–350	0.0037 ± 0.0007 (stat.) ± 0.0002 (sys.)	0.004331 +- 0.0006(stat.) +- 0.0001(sys.)

Appendix. Paper CS

x range	$\frac{d\sigma}{dx}$ (pb)	New CS
0.0002–0.001	4869 ± 334 (stat.) ± 312 (sys.)	5029.56 +- 365.8311(stat.) +- 300.3509(sys.)
0.001–0.003	1811 ± 139 (stat.) ± 104 (sys.)	1858.06 +- 148.0170(stat.) +- 119.9582(sys.)
0.003–0.01	278 ± 31 (stat.) ± 13 (sys.)	280.517 +- 31.3222(stat.) +- 15.6644(sys.)
0.01–0.02	25 ± 7 (stat.) ± 3 (sys.)	28.8137 +- 6.4689(stat.) +- 1.8541(sys.)

E_T^{jet} range (GeV)	$\frac{d\sigma}{dE_T^{\text{jet}}}$ (pb GeV^{-1})	New CS
2.5–4	1.40 ± 0.16 (stat.) ± 0.08 (sys.)	1.394510 +- 0.1801(stat.) +- 0.0721(sys.)
4–6	1.19 ± 0.11 (stat.) ± 0.10 (sys.)	1.242430 +- 0.1137(stat.) +- 0.0884(sys.)
6–8	1.01 ± 0.10 (stat.) ± 0.07 (sys.)	1.011080 +- 0.1006(stat.) +- 0.0660(sys.)
8–10	0.74 ± 0.07 (stat.) ± 0.05 (sys.)	0.778383 +- 0.0734(stat.) +- 0.0434(sys.)
10–15	0.32 ± 0.03 (stat.) ± 0.02 (sys.)	0.316250 +- 0.0334(stat.) +- 0.0088(sys.)
15–35	0.031 ± 0.006 (stat.) ± 0.003 (sys.)	0.031535 +- 0.0052(stat.) +- 0.0052(sys.)

η^{jet} range	$\frac{d\sigma}{d\eta^{\text{jet}}}$ (pb)	New CS
−1.5 to −0.7	1.53 ± 0.17 (stat.) ± 0.15 (sys.)	1.668240 +- 0.1760(stat.) +- 0.1654(sys.)
−0.7–0.1	2.84 ± 0.25 (stat.) ± 0.19 (sys.)	3.090260 +- 0.2576(stat.) +- 0.2000(sys.)
0.1–0.9	3.91 ± 0.33 (stat.) ± 0.14 (sys.)	4.034600 +- 0.3502(stat.) +- 0.1574(sys.)
0.9–1.8	3.57 ± 0.29 (stat.) ± 0.22 (sys.)	3.461140 +- 0.3030(stat.) +- 0.2022(sys.)

Appendix. Studied fits

- A bin by bin $min\chi^2$-fitting procedures is done. The minimized functions:
  1. $\boldsymbol{Data - Photons_{MC} * a - Background_{MC} * (1-a)}$
  2. $\boldsymbol{Data - LL_{MC} - QQ_{MC} * a - Background_{MC} * (1-a)}$
  3. $\boldsymbol{Data - QQ_{MC} * a - Background_{MC} * (1-a)}$
  4. $\boldsymbol{Data - QQ_{MC} * a - Background'_{MC} * (1-a)}$
- Number of fitted photons is defined:
  - $\boldsymbol{N = a * Ndata_{,full} * \frac{N_{sg,full}}{N_{sg,fitted}} + NLL_{,full}}$ for (1) and (2)
  - $\boldsymbol{N = a * Ndata_{,full} * \frac{N_{sg,full}}{N_{sg,fitted}}}$ for (3) and (4)

* $\boldsymbol{Background_{MC}}$ - hadronic background

**$\boldsymbol{Background'_{MC}}$- hadronic background and $\boldsymbol{LL_{MC}}$

***$\boldsymbol{Photons_{MC}}$ - $\boldsymbol{QQ_{MC}}$ and $\boldsymbol{LL_{MC}}$

Δφ bin-by-bin fit

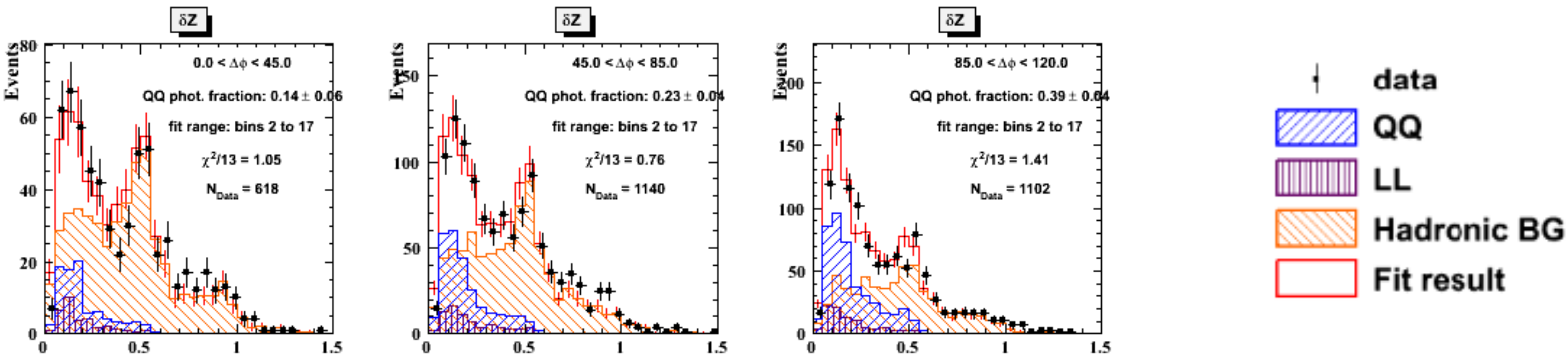

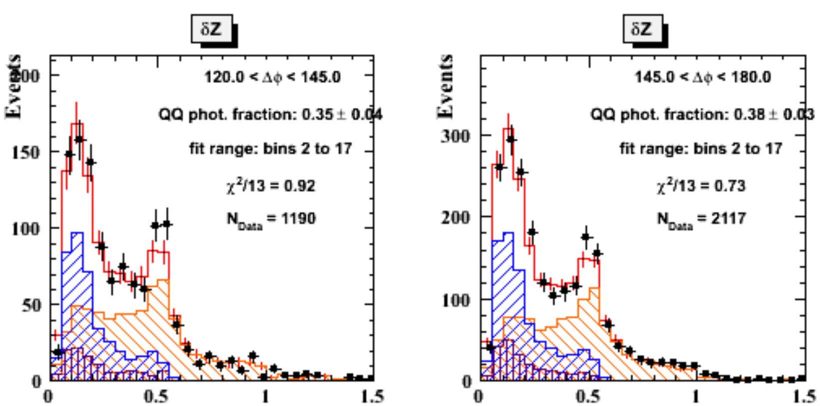

For **data = LL' + QQ' * a + bg' * (1-a)**
fitting with Ian's correction .

Across all the types of fitting the differences in calculated parameters are ~1-2%

Appendix.Comparison of fits

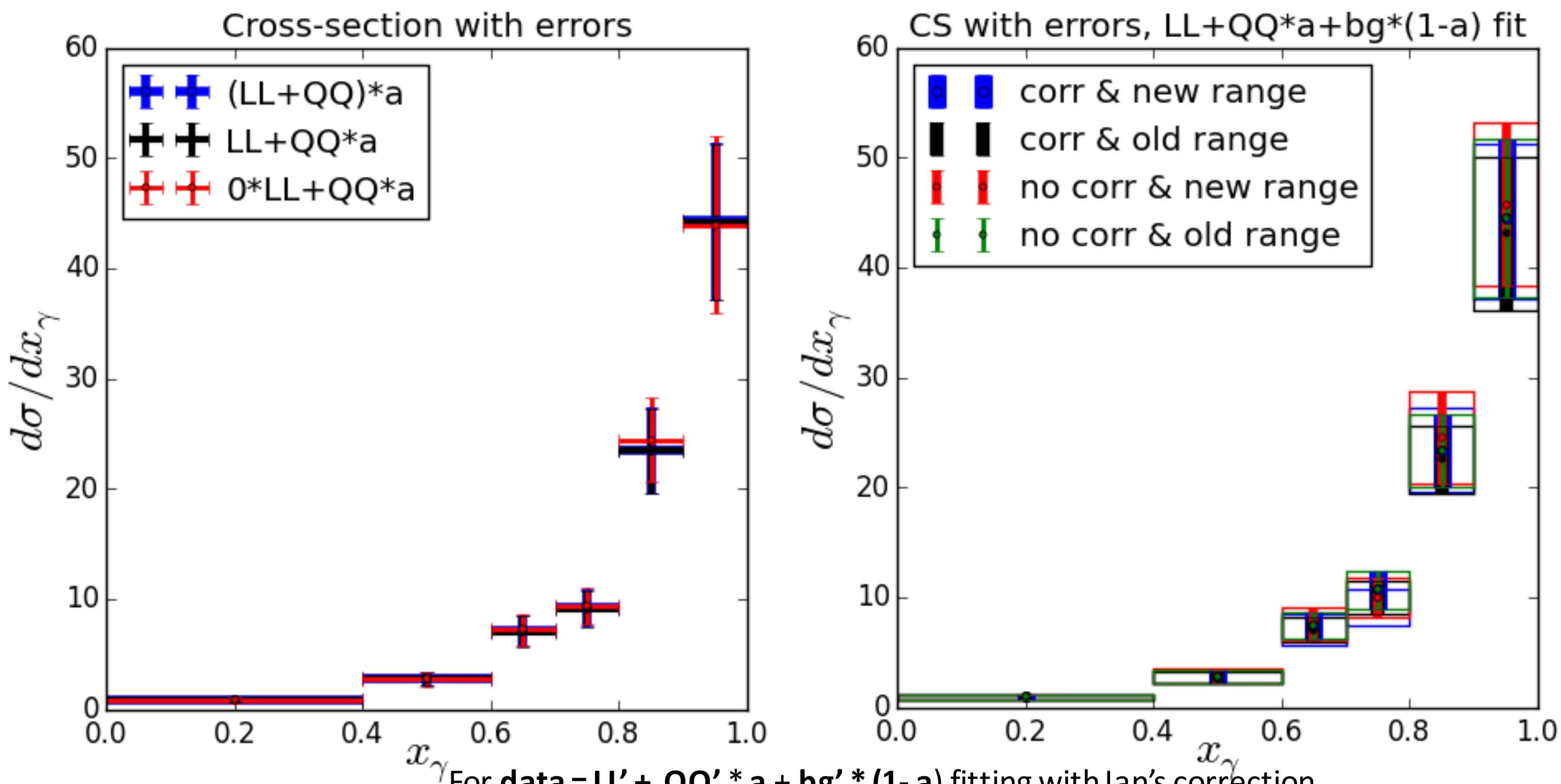

For **data = LL' + QQ' * a** + **bg' * (1- a**) fitting with Ian's correction .